COMPARISON OF THE BOUNDARY ELEMENT METHOD AND THE METHOD OF FUNDAMENTAL SOLUTIONS FOR ANALYSIS OF POTENTIAL AND ELASTICITY PROBLEMS IN CONVEX AND CONCAVE DOMAINS

SORAYA ZENHARI[1], MOHAMMAD RAHIM HEMATIYAN[2], AMIR KHOSRAVIFARD[2] & HANS-CHRISTIAN MÖHRING[1]
[1]Institut für Werkzeugmaschinen (IfW), Universität Stuttgart, Germany
[2]Mechanical Engineering Department, Shiraz University, Iran
[3]Civil and Environmental Engineering Department, Shiraz University, Iran

ABSTRACT
The boundary element method (BEM) and the method of fundamental solutions (MFS) are well-known fundamental solution-based methods for solving a variety of problems. Both methods are boundary-type techniques and can provide accurate results. In comparison to the finite element method (FEM), which is a domain-type method, the BEM and the MFS need less manual effort to solve a problem. The aim of this study is to compare the accuracy and reliability of the BEM and the MFS. This comparison is made for 2D potential and elasticity problems with different boundary and loading conditions. In the comparisons, both convex and concave domains are considered. Both linear and quadratic elements are employed for boundary element analysis of the examples. The discretization of the problem domain in the BEM, i.e., converting the boundary of the problem into boundary elements is relatively simple; however, in the MFS, obtaining appropriate locations of collocation and source points need more attention to obtain reliable solutions. The results obtained from the presented examples show that both methods lead to accurate solutions for convex domains, whereas the BEM is more suitable than the MFS for concave domains.
Keywords: boundary element method, method of fundamental solutions, elasticity, potential problem, convex domain, concave domain.

1 INTRODUCTION

Numerical methods developed for solving partial differential equations can be divided into two basic categories namely domain-type and boundary-free methods. Among domain-type methods, one can mention the finite element method (FEM), the finite difference method, and the finite volume method. The main advantages of boundary-type methods over domain-type methods are their fewer amounts of input data and their potential to tackle with moving boundaries, moving loads, and infinite domains. Over last three decades, engineers and scientists have become more interested in mesh reduction methods. Computational methods such as the boundary element method (BEM) and the method of fundamental solutions (MFS) are among these techniques and both are capable of providing excellent results for solving different problems in physics and engineering [1], [2]. The two methods are based on the knowledge of a fundamental solution of the problem. However, unlike the BEM, the MFS is an integration-free method and has some attractiveness for solving some problems [2], [3]. The MFS reduces the computation time significantly in comparison with the BEM as it does not require boundary discretization and computation of singular or regular integrals over the boundary [4], [5] and it can solve certain inverse problems without iteration [6]. Primarily research on the BEM for potential problems dates back to 1903 when Fredholm established his investigation on potential problems based on a discretization technique. The direct boundary integral equation for potential problems was first proposed by Jaswon [7] and Symm [8]. The BEM for solving potential problems in axisymmetric domains was

WIT Transactions on Engineering Sciences, Vol 135, © 2023 WIT Press
www.witpress.com, ISSN 1743-3533 (on-line)
doi:10.2495/BE460081

successfully established by Rizzo and Shippy [9]. Earlier attempts to use the BEM for elasticity problems was made by Muskhelishvili et al. [10], Kupradze [11]. After that, the BEM was employed for analysis of a wide range of problems.

The idea of the MFS as a computational tool for solving various partial differential equations dates back to 1960s where Kupradze and Aleksidze [12] introduced this method for boundary value problems and later Mathon and Johnston [13] improved this method for numerical implementation. Karageorghis and Fairweather [14] employed the MFS for axisymmetric potential problems for the first time. Later, it was successfully applied to a variety of potential and elastic problems, see for example Fam and Rashed [15], Young et al. [16], Marin et al. [17], Karageorghis et al. [18], Fan and Li [19], Mohammadi et al. [20]. Suitable arrangement of source points and collocation points in the MFS has been always disputable and under discussion among the researchers. An arrangement of collocation points in the MFS can lead to an accurate solution while another arrangement with a little change may lead to inaccurate results [21]. In the MFS, the location of the pseudo boundary can be fixed and selected before solving the problem, or it may be determined by an optimization process. In former case, a pseudo boundary similar to the boundary of the problem is usually considered [22]–[24]. In the latter case, the optimal pseudo boundary as a circle and a sphere in 2D and 3D problems is found, respectively [25]–[27]. Optimal pseudo boundaries can provide more accurate solutions [28]–[30]; however, it should be mentioned that optimization algorithms can be relatively time consuming [27] and disappear the simplicity and attractiveness off the MFS. Recently, Hematiyan et al. have recommended some remarks for properly determination of the position of source points in the MFS for potential [3] and elasticity [31] problems. In previous investigations, the BEM and the MFS have been compared in some aspects. Tadeu et al. [32] investigated the efficiency of the BEM, the MFS and radial basis function (RBF) method in wave propagation problem in an elastic domain. The MFS was found to provide results with more accuracy. Salgado-Ibarra [33] compared the accuracy of the MFS and the BEM for an elliptical domain considering different boundary conditions. A circle was considered as the pseudo boundary for solving the Laplace equation and the Saint Venant's torsion problem using the MFS. They observed that the MFS was less time-consuming and had much easier implementation. Alves et al. [34] applied the BEM and the MFS to 2D Laplace equation. The accuracy of these methods was studied for several problems with discontinuity of boundary conditions. They observed that the BEM with double layer potential has a better performance in comparison with the MFS for problems with discontinuous boundary conditions. Considering different computational fields like magnetic and electric problems the scientist obtained similar observations, which acknowledged the superiority of the MFS over the BEM for some cases [35], [36]. Similar to the BEM, the MFS technique can be particularly useful for the analysis of acoustic problems, Godinho et al. [37] and Godinho and Soares [38] while the formulation of the MFS is simpler than the BEM. Dyhoum et al. [39] investigated several EIT (electrical impedance tomography) problems and found the BEM more convergent and stable in comparison with the MFS, which imposed some restriction on the arrangement of source points. Liravi et al. [40] analysed elastodynamics behaviour of solid structure, e.g., cylinder and a thin circular shell located in the soil. A new control technique was implemented to discover the optimal distance between collocation points. According to this investigation, the MFS showed a greater sensitivity to the parameters than the BEM.

In this study, the MFS and the direct BEM for solving potential and elasticity problems in 2D convex and concave domains are compared. By performing numerical studies, the advantages and disadvantages of the two methods for convex and concave domains with simple and complicated boundary conditions are highlighted. To the authors' best knowledge, it is the first time that the ability of the MFS and the BEM for different shapes of domain are compared.

2 THE MFS AND THE BEM FOR POTENTIAL AND ELASTOSTATIC PROBLEMS

2.1 The MFS for potential problems

In the MFS for 2D problems, some collocation points must be considered on the physical boundary of the problem in order to satisfy the boundary conditions, followed by source points on the pseudo boundary, which is defined around the physical boundary. Any source point placed on the pseudo boundary corresponds to a fundamental solution, which provides a solution. Due to linearity of the Laplace and elasticity equations, the summation of the fundamental solutions with arbitrary coefficients also satisfies the equations. The coefficients (intensities of sources) can be determined by satisfying the boundary conditions of the problem at the collocation points. This procedure generates a system of equations, solution of which provides the unknown coefficients. The number of unknowns and the number of equations is in accordance with the number of source points and collocation points, respectively. The solution for an arbitrary internal or boundary point can be found by taking into account the effects of all sources on the pseudo boundary. The Laplace's equation in the 2D domain Ω with a generalized boundary condition on the boundary Γ are expressed as follows:

$$\nabla^2\phi = 0 \quad \text{in} \quad \Omega, \tag{1}$$

$$f_1\phi + f_2\frac{\partial\phi}{\partial n} = f_3 \quad \text{on} \quad \Gamma, \tag{2}$$

where, f_1, f_2 and f_3 are known functions on the boundary, n is the outward direction normal to the boundary Γ and ϕ is the primary variable of the problem. As previously mentioned, the solution is approximated by a linear combination of fundamental solutions as follows [14]:

$$\phi(\boldsymbol{x}) = \sum_{i=1}^{N} a_i\phi^*(\boldsymbol{x}, \boldsymbol{\xi}_i), \tag{3}$$

where a_i and $\boldsymbol{\xi}_i$ represent the intensity and location of the ith source located on the pseudo-boundary Γ', N is the number of source points, and $\boldsymbol{x}$ is the coordinate of the point in the domain or on the boundary of the solution domain. The constants a_i are the unknowns of the problem that have to be found. The fundamental solution for 2D Laplace equation can be expressed as follows [41]:

$$\phi^*(\boldsymbol{x}, \boldsymbol{\xi_i}) = -\frac{1}{2\pi}\ln r_i, \tag{4}$$

where r_i represents the distance between the source point $\boldsymbol{\xi_i}$ and the field point $\boldsymbol{x}$. Substituting eqn (4) into eqn (3) leads to:

$$\sum_{i=1}^{N} a_i\left[f_1(\boldsymbol{C_j})\phi^*(\boldsymbol{C_j}, \boldsymbol{\xi_i}) + f_2(\boldsymbol{C_j})\frac{\partial\phi^*(\boldsymbol{C_j}, \boldsymbol{\xi_i})}{\partial n}\right] = f_3(\boldsymbol{C_j}), \quad j = 1, 2, ..., M, \tag{5}$$

where $\boldsymbol{C_1}, \boldsymbol{C_2}, ..., \boldsymbol{C_M}$ are collocation points. In order to find the unknowns of the problem i.e., a_i, the number of the equations or collocation points should be greater than the number of unknowns or source points ($M \geq N$). Eqn (5) indicates a system of M linear equations with N unknowns, which can be written in following form:

$$\mathbf{BX} = \mathbf{F}, \tag{6}$$

where the elements of the matrix $\mathbf{B} \in (\boldsymbol{R}^{M\times N}$, the vectors $\mathbf{X} \in \boldsymbol{R}^N$ and $\mathbf{F} \in \boldsymbol{R}^M$ can be expressed as:

$$B_{ji} = f_1(\boldsymbol{C_i})\phi^*(\boldsymbol{C_i}, \boldsymbol{\xi_j}) + f_2(\boldsymbol{C_j})\frac{\partial \phi^*(\boldsymbol{C_i}, \boldsymbol{\xi_j})}{\partial n}, \tag{7}$$

$$F_i = f_3(\boldsymbol{C_i}), \quad X_i = a_i. \tag{8}$$

In the case of $M = N$, the system of equations can be solved using standard methods such as the Gaussian elimination method or using the inverse of the coefficient matrix as follows:

$$\mathbf{X} = \mathbf{B^{-1}F}. \tag{9}$$

In the case of $M > N$, the system of equations will be over-determined and can be solved in the least-squares sense as follows:

$$\mathbf{X} = (\mathbf{B}^T\mathbf{B})^{-1}\mathbf{B}^T\mathbf{F}. \tag{10}$$

When the intensity of the source points a_i are determined, the solution can be calculated on any internal or boundary points using eqn (3).

2.2 The direct BEM for Laplace's equation

The BEM is based on the Green theorem where the fundamental solution of the Laplace equation is taken as the auxiliary function. Two scalar functions ϕ^* and ϕ which are continuous over the domain boundary are considered in the BEM that correspond to the fundamental solution of the Laplace equation and the variable of the problem, respectively. Using the Green theorem, the integral equation for the Laplace's equation can be expressed as follows [41]:

$$\int_\Omega (\phi(\boldsymbol{z})\nabla^2\phi^*(\boldsymbol{x}, \boldsymbol{z}) - \phi^*(\boldsymbol{x}, \boldsymbol{z})\nabla^2\phi(\boldsymbol{z}))dv(\boldsymbol{z}) = \int_\Gamma (\phi(\boldsymbol{y})\ \frac{\partial \phi^*}{\partial n}(\boldsymbol{x}, \boldsymbol{y}) - \phi^*(\boldsymbol{x}, \boldsymbol{y})\ \frac{\partial \phi}{\partial n}(\boldsymbol{y}))ds(\boldsymbol{y}), \quad \boldsymbol{x}, \boldsymbol{z}\ \in \Omega, \boldsymbol{y} \in \Gamma. \tag{11}$$

The function ϕ corresponds to the variables of the problem defined on the domain Ω, ϕ^* is fundamental solution of the Laplace equation which is defined according to eqn (4) and n is the outward normal direction to the boundary. The point $\boldsymbol{x}$ in this equation corresponds to the location of a unit load in the auxiliary problem, while $\boldsymbol{y}$ and z are arbitrary points on or within the boundary of the problem. Eqn (11) can be simplified by using the Green theorem and integration techniques as follows [41]:

$$c(\boldsymbol{x})\phi(\boldsymbol{x}) + \int_\Gamma \phi(\boldsymbol{y})\frac{\partial \phi^*}{\partial n}(\boldsymbol{x}, \boldsymbol{y})ds(\boldsymbol{y}) = \int_\Gamma \phi^*(\boldsymbol{x}, \boldsymbol{y})\frac{\partial \phi}{\partial n}\boldsymbol{y})ds(\boldsymbol{y}),\ \boldsymbol{x}, \boldsymbol{y} \in\ \Gamma. \tag{12}$$

$c(\boldsymbol{x})$ is a coefficient which presents the free term of integral equation and it will be calculated according to the geometry and boundary condition of the problem [41].

2.3 The MFS for 2D elastostatic problems

When there are no body forces, the governing equations for the elastostatic problem in 2D domain Ω and its boundary Γ are expressed as follows [42]:

$$\sigma_{ij,j} = 0, \tag{13}$$

$$\varepsilon_{ij} = \frac{1}{2}\left(u_{i,j} + u_{j,i}\right), \tag{14}$$

$$\sigma_{ij} = \frac{\nu E}{(1+\nu)(1-2\nu)}\delta_{ij}\varepsilon_{kk} + \frac{E}{1+\nu}\varepsilon_{ij}, \tag{15}$$

where σ_{ij} and ε_{ij} are the stress and strain tensors, respectively; u_i is the displacement vector, ν and E are the Poisson's ratio and Young module of the problem. The boundary condition for general 2D elastostatic problems can be expressed as:

$$f_{sj}u_j + g_{si}\sigma_{ij}n_j = p_s, \quad i, j, s = 1, 2 \qquad \text{for 2D problems.} \tag{16}$$

f_{sj}, g_{si} and p_s are given functions on the boundary and n_j represent components of the outward unit vector normal to the boundary Γ. In the MFS for elastostatic problems, displacement components are generally explained as follows [14]:

$$u_i(\boldsymbol{x}) = \sum_{k=1}^{N}\sum_{m=1}^{2} a_m(\boldsymbol{\xi_k})u^*_{im}(\boldsymbol{x}, \boldsymbol{\xi_k}), \tag{17}$$

where ξ_k is the location of the kth source (concentrated fictitious force) located on the pseudo-boundary Γ', N is the number of source points, and $\boldsymbol{x}$ is a point in the domain or on the boundary of the solution domain. The constants $a_m(\xi_i)$ are the unknowns of the problem, which must be determined. The strain tensor components are obtained by substituting eqn (17) into (14), which yields:

$$\varepsilon_{ij}(\boldsymbol{x}) = \sum_{k=1}^{N}\sum_{m=1}^{2} a_m(\boldsymbol{\xi_k})\varepsilon^*_{ijm}, \tag{18}$$

where

$$\varepsilon^*_{ijm} = \frac{u^*_{im,j} + u^*_{jm,i}}{2}. \tag{19}$$

In addition, the stress tensor components may also be computed by substituting eqn (18) into eqn (15):

$$\sigma_{ij}(\boldsymbol{x}) = \sum_{k=1}^{N}\sum_{m=1}^{2} a_m(\boldsymbol{\xi_k})\sigma^*_{ijm}, \tag{20}$$

where

$$\sigma^*_{ijm} = \left[\frac{\nu E}{(1+\nu)(1-2\nu)}\delta_{ij}u^*_{tm,t} + \frac{E}{2(1+\nu)}(u^*_{im,j} + u^*_{jm,i})\right]. \tag{21}$$

To calculate the stress and strain components, the first derivatives u^*_{ij} must also be calculated. The fundamental solution for 2D elasticity problems is given as follows [22]:

$$u^*_{ij} = \frac{1}{8\pi G(1-\bar{\nu})}\left[(3-4\bar{\nu})\delta_ijln\frac{1}{r} + r_{,i}.r_{,j}\right], \quad i, j = 1, 2. \tag{22}$$

The term r refers to the distance between source and any point within the domain or on its boundary and G is the shear module. $\bar{\nu}$ for plane strain problems is the same as ν while for plane stress problems is $\frac{\nu}{(1+\nu)}$. Differentiating eqn (22) leads to:

$$u^*_{ij,k} = \frac{1}{8\pi G(1-\bar{\nu})}\left[-(3-4\bar{\nu})\frac{r_k}{r^2}\delta_i j + \frac{r_j}{r^2}\delta_j k - \frac{2r_i r_j r_k}{r^4}\right], \quad i,j,k = 1,2, \tag{23}$$

where

$$r_i = x_i - \xi_i, r_{,i} = \frac{\partial r}{\partial x_i} = \frac{r_i}{r}, \qquad r = \sqrt{(x_1-\xi_1)^2 + (x_2-\xi_2)^2}, \tag{24}$$

$$\xi_2 = \eta\xi_1 = \xi, \quad x_2 = y, \quad x_1 = x, \tag{25}$$

$$r = \sqrt{(x-\xi)^2 + (y-\eta)^2}. \tag{26}$$

After substituting eqns (17) and (20) into (16) for an arbitrary boundary point M, the following equation is obtained:

$$\sum_{k=1}^{N}\sum_{m=1}^{2} a_m(\boldsymbol{\xi_k})[f_{sj}(\boldsymbol{C_l})u^*_{jm}(\boldsymbol{C_l},\boldsymbol{\xi_k}) + g_{si}(\boldsymbol{C_l})\sigma^*_{ijm}(\boldsymbol{C_l},\boldsymbol{\xi_k})n_j] = p_s(\boldsymbol{C_l}),$$
$$l = 1,2,...,M. \tag{27}$$

According to eqn (27), for 2D case, there will be 2M equations with 2N unknowns, in which M and N are collocation and source points, respectively. $C_1, C_2, ..., C_M$ in eqn (27) are collocation points. In order to obtain the unknowns $a_m(\xi_i)$, the number of equations should be equal or greater than the unknowns ($2N \geq 2M$). Eqn (27), which shows the system of 2M equations with 2N unknowns, can be written in the form of:

$$\mathbf{BX} = \mathbf{F}. \tag{28}$$

When $M = N$, the system of equations in eqn (24) can be solved as $\mathbf{X} = \mathbf{B^{-1}F}$. In the case of $M > N$ the system of equations should be solved using least-square method as $\mathbf{X} = (\mathbf{B^TB})\mathbf{B^TF}$. By calculating the coefficient of sources, solution in any arbitrary point inside the domain or on the boundary can be achieved using eqn (22).

2.4 The direct BEM for 2D elastostatic problems

The reciprocal theorem is used to derive integral equations of elasticity. Assume that an elastic body is subjected to two different loads and the solutions of the two problems are numbered (1) and (2), respectively. This theorem indicates that the work done by the first system of work acting via displacement of the second system is equal to the work done by the second system of forces acting via displacement of the first system, that is [42]:

$$\int_\Gamma t_i{}^{(1)}u_i{}^{(2)}d\Gamma + \int_\Omega F_i{}^{(1)}u_i{}^{(2)}d\Omega = \int_\Gamma t_i{}^{(2)}u_i{}^{(1)}d\Gamma + \int_\Omega F_i{}^{(2)}u_i{}^{(1)}d\Omega, \tag{29}$$

where F_i and t_i represent body force and traction components, respectively. Using the reciprocity theorem, one can obtain the elasticity integral equation. This is done by considering the main problem as the first system and the Kelvin problem with the fundamental solution as the second one. The integral equation of elasticity in the absence of body force and in a boundary form can be written as follows [41]:

$$c_{ji}(\boldsymbol{x})u_i(\boldsymbol{x}) + \int_{\Gamma} u^*_{ij}(\boldsymbol{x},\boldsymbol{y})u_i(\boldsymbol{y})ds(\boldsymbol{y}) = \int_{\Gamma} T^*_{ij}(\boldsymbol{x},\boldsymbol{y})t_i(\boldsymbol{y})ds(\boldsymbol{y}), \;\; \boldsymbol{x},\boldsymbol{y} \in \Gamma, \tag{30}$$

where u^*_{ij} represents the displacement fundamental solution of elasticity and is given in eqn (22) and c_{ji} are free term coefficients [43]. T^*_{ij} is expressed as follows [41]:

$$T^*_{ij} = \frac{-1}{4\pi(1-\bar{\nu})r}\left[\frac{\partial r}{\partial n}[(1-2\bar{\nu})\delta_{ij} + 2r_{,i}.2r_{,j}] - (1-2\bar{\nu})(r_i n_j - r_j n_i)\right]. \tag{31}$$

The component of stress after discretizing the boundary of the domain with a number of boundary elements and after some numerical manipulations, the discretized form of the boundary element equation may be written in matrix form as:

$$Hu = Gt. \tag{32}$$

After satisfying the prescribed boundary conditions and rearrangement of unknowns (displacement or traction) a standard system of algebraic equations is obtained that can be solved by standard system solving methods.

2.5 A suitable configuration for source points in the MFS for 2D elasticity

The arrangement of source and collocation points has considerable effects on the accuracy of the MFS results. In some problems, a little change in the configuration of source points may lead to a considerable error in the results. Although extensive studies have been conducted on the location of source points in the MFS, investigation on this topic is still underway. In this work, we select the location of source points based on the recommendations provided by Hematiyan et al. [3], [31]. According to the suggestion of Hematiyan et al. [3], the positions of source points in the 2D potential problem is determined in such a way that the value of the location parameter of the source points would be greater than 0.8. The value of the location parameter in the 2D elastostatic problem is recommended to be greater than 0.85. The value of the location parameter determines the location of an individual source point relative to its neighboring source points and the boundary of the problem. The location parameter can be defined using Fig. 1, which shows the schematic view of the main boundary, the pseudo boundary and source points. The closest boundary point to the ith source point $\mathbf{S}_i$ is considered as its base point and is donated by $\mathbf{B}_i$.

The location parameter is defined as follows:

$$K_i = \frac{d_{i/i}}{max(d_{i-1/i}, d_{i+1/i})}, \quad 0 < K_i < 1. \tag{33}$$

where $d_{i/j}$ represents the distance between the base point $\mathbf{B}_j$ to the source point $\mathbf{S}_j$. If the location parameter has a small value (the source points are close to the boundary), the solutions will have an oscillation, while a larger value (near to 1.0) of the location parameter (source points are far from the boundaries) will result in ill-conditioned system of equations.

3 RESULTS AND DISCUSSION

In this section by presenting several numerical examples with different geometries and boundary conditions, the accuracy of the BEM and the MFS for convex and concave domains are compared.

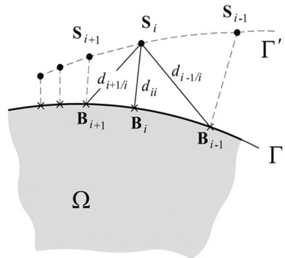

Figure 1: The location of a source point relative to the base points of the neighboring source points [3].

Table 1: Comparing temperature values in BEM and MFS for a Dirichlet boundary condition for a rectangular sheet.

Node numbers	T_{MFS}	T_{BEM}
24	2.17662	2.286
54	2.1755	2.179
100	2.1755	2.176
Reference solution	2.1755	2.1755

3.1 Comparison of the BEM and the MFS for potential problems

3.1.1 A rectangular plate with Newmann boundary condition

A rectangular domain (2×1) is considered with a coordinate system located at the center of the rectangle. There are the following boundary conditions for the Laplace equation to be solved:

$$\phi = x^2 + y^2 \qquad \text{on} \quad \Gamma. \tag{34}$$

The problem has been solved using BEM and MFS with 24, 56, and 100 nodes. The MFS configuration for the three cases is shown in Fig. 2. All three of these cases show a magnitude of 0.9 for the location parameter. In the boundary element nodes are located on the boundary at the same distance. A reference point of (1.25,0) is specified between BEM and MFS for comparison purposes. A reference solution was obtained using the finite element method with appropriate grid numbers. Table 1 provides the results for all three methods with different node numbers. According to a reference solution, both methods are capable of providing a reliable solution, and increasing the number of nodes will increase accuracy. While both methods are acceptable in accuracy, it's apparent that the MSF is more accurate with a lower number of nodes.

3.1.2 Sheet plate with concave domain

This example illustrates how geometrical complexity of the domain affects the accuracy of the solution obtained from MFS and BEM. Fig. 3 illustrates the plate with a concave domain and boundary conditions. The boundary conditions and the governing equation of the sheet

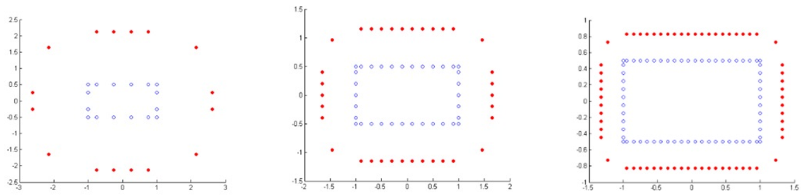

(a) (b) (c)

Figure 2: MFS arrangement of source and collocation points for a rectangular sheet with the number of (a) 24; (b) 54; (c) 100 nodes.

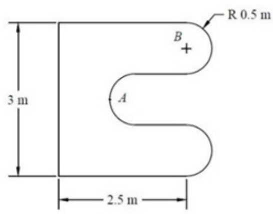

Figure 3: Concave sheet.

Table 2: A comparison of temperature and flux values at Point A in a concave sheet domain.

Node numbers	T_{MFS}	T_{BEM}	$TG_{x(BEM)}$	$TG_{x(MFS)}$
35	3.250	3.249	1.0458	1.0245
67	3.250	3.249	1.0267	1.0270
90	3.250	3.250	1.0250	1.0285
Reference solution	3.250	3.250	1.0275	1.0275

are as follows:

$$T = x^2 + y^2 \qquad \text{on the boundary,} \tag{35}$$

$$\nabla^2 T = 0 \qquad \text{inside the domain.} \tag{36}$$

Temperature and flux at two arbitrary points A (1, 1.5) and B (2.5, 2.5) are calculated in order to compare the accuracy of the proposed methods. The accuracy of the problem is examined using 35, 67, and 90 nodes. Based on these values, BEM and MFS solutions were compared. Finite element software is used to obtain reference values for flux and temperature at points A and B. Tables 2 and 3 provide the calculated values of temperature and flux at points A and B.

For BEM (Fig. 4), all nodes are located at the same distance from the boundary, while for MFS (Fig. 5), the distance between nodes at the corner is smaller than for other nodes, this distance will be achieved using location parameter.

Table 3: A comparison of temperature and flux values at Point B in a concave sheet domain.

Node numbers	T_{MFS}	T_{BEM}
35	12.875	12.865
67	12.871	12.868
90	12.870	12.868
Reference solution	12.870	12.870

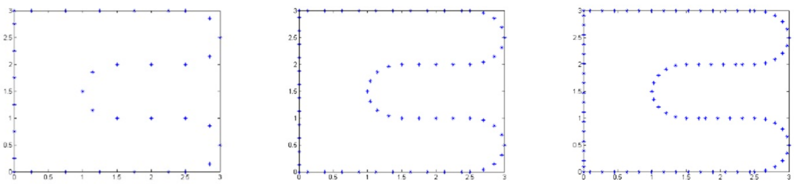

(a) (b) (c)

Figure 4: A BEM with (a) 35; (b) 67; and (c) 90 nodes for concave sheet plate.

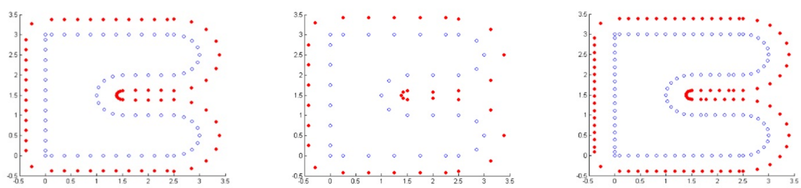

(a) (b) (c)

Figure 5: MFS arrangement of source points and collocation points with (a) 35; (b) 67; and (c) 90 nodes.

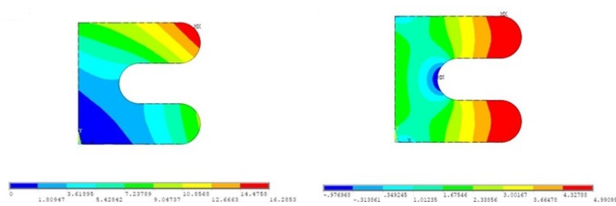

(a) (b)

Figure 6: (a) Temperature contours; and (b) Flux contours in concave sheet plate in FEM.

A reference solution for temperature and flux is calculated and simulated using finite element software. Figs 6 and 7 represent the temperature and flux contours, respectively.

It has been necessary to calculate the temperature and flux contours obtained from MFS in order to gain a more comprehensive understanding of the results. The contours of temperature

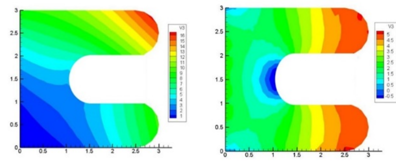

(a) (b)

Figure 7: (a) Temperature contours; and (b) Flux contours in concave sheet plate in MFS.

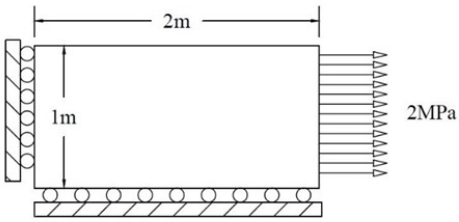

Figure 8: The rectangular plate with plane strain condition.

and flux are shown in Fig. 8. As can be seen, the solution calculated by MFS on the domain of the problem is similar to the reference solution calculated by finite element software.

Clearly, both BEM and MFS can provide high accuracy results for both temperature and flux fields. The accuracy of both methods is the same, and the convergence rate to the reference solution is increased by increasing the number of nodes. The FEM method requires the use of thousands of nodes for fine-meshing, while the MFS and BEM methods can achieve high accuracy results with only 90 nodes. As an alternative to MFS, BEM can provide more accurate solutions in a concave domain, not only at point A, but also at internal point B. As a result, it can be concluded that the arrangement of source points and collocation points in MFS is critical. It is preferred to use BEM in cases of geometric complexity in which a suitable arrangement of source points and collocation points cannot be achieved.

3.2 Comparison of BEM and MFS for elasticity problems

3.2.1 Rectangular plate with plane strain condition

In this study, a rectangular sheet plate with roller support on two sides was considered, and the results of BEM and MFS were compared when a distributed tension load of 2 MPa was applied. Fig. 8 illustrates the geometry, loading, and boundary conditions of the problem. In solving the problem, Young's module ($E = 2 \times 10^9$) and Poisson's ratio ($\nu = 0.3$) were considered. Different numbers of source points were used to solve the problem, namely 24, 48, and 96. As a result of the study, error percentages for each method were calculated. It is necessary to determine the appropriate location for source points and collocation points. Based on evaluations, the location parameter of 0.85 has been chosen. Fig. 9 illustrates the configuration for source points and collocation points in MFS. In BEM, the arrangements of boundary nodes are presented in Fig. 10 with different numbers of boundary nodes. We should remember that despite MFS, nodes can be positioned at the corner of a rectangular

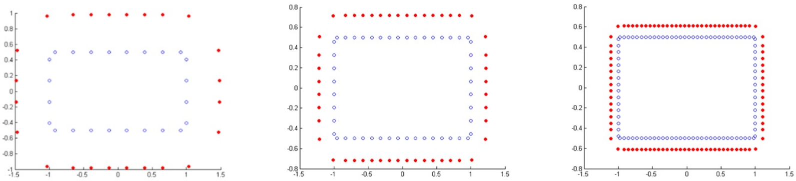

(a) (b) (c)

Figure 9: Arrangement of source points and collocation points for a rectangular plate with plane strain condition in MFS with number of (a) 24; (b) 48; and (c) 98 nodes.

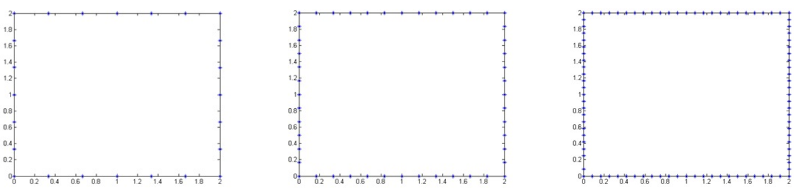

(a) (b) (c)

Figure 10: Arrangement boundary node for a rectangular plate with plane strain condition in BEM with number of (a) 24; (b) 48; and (c) 98 nodes.

Table 4: Percentage of displacement error in MFS and BEM for rectangular sheet.

Node numbers	$E_{ux(MFS)})$	$E_{ux(BEM)}$	$E_{uy(MFS)}$	$E_{uy(BEM)}$
24	23.6×10^{-4}	0.26×10^{-4}	17.17×10^{-4}	0.24×10^{-4}
48	20.8×10^{-4}	0.18×10^{-4}	10.9×10^{-4}	0.146×10^{-4}
96	1.28×10^{-4}	0.13×10^{-4}	0.43×10^{-4}	0.0096×10^{-4}

plate in BEM as well. In the case of plain stress conditions, the displacement formulation provides an accurate solution.

As shown in Table 4, the mean error is calculated for each method with different numbers of nodes, the indices ux and uy indicate the horizontal and vertical displacements, respectively. The results indicate that both methods provide accurate and precise answers. With an increase in the number of nodes, the accuracy of the solutions will also increase. Despite the fact that the rate of error for the two methods is practically negligible, the accuracy or robustness of the BEM method has a distinct advantage over the fundamental solution method. solution method.

3.2.2 A plate with a deep hole

Following the previous problem, the hole within the sheet has deepened, and the stress values at points A and B will be analyzed. Fig. 11 presents the boundary conditions and geometry of the example.

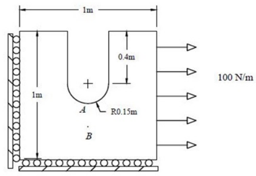

Figure 11: Plate with much deeper hole.

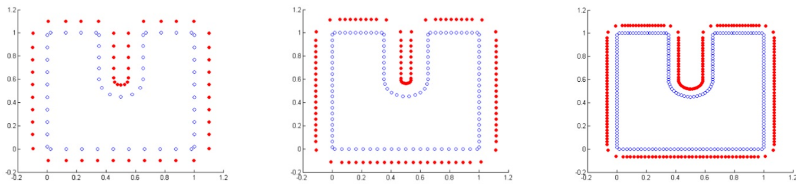

(a) (b) (c)

Figure 12: Arrangement of source points and collocation points for a plate with a deep hole with number of (a) 50; (b) 111; and (c) 213 nodes in MFS.

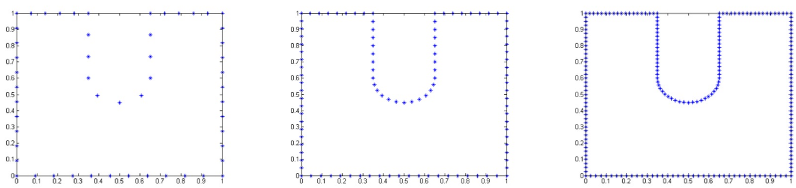

(a) (b) (c)

Figure 13: Arrangement of boundary nodes for a plate with a deep hole with number of (a) 50; (b) 111; and (c) 213 nodes in BEM.

Based on finite element software, a reference solution of stresses at points A and B has been obtained. According to MFS, the appropriate arrangement of source and collocation points yields a position parameter of 0.85 approximately. To solve this example, both methods consider three distinct node arrangements, namely 53, 111, and 213 nodes. Figs 12 and 13 illustrate the arrangement of points in the BEM and MFS respectively. In MFS, it should be noted that no nodes are placed in corners. Tables 5 and 6 provide a comparison between BEM and MFS results at point A and B. In order to determine the efficacy of BEM, two types of elements were used namely linear and quadratic.

It can be seen from Tables 5 and 6 that BEM has superiority over MFS, particularly when considering quadratic elements. Several configurations were examined to determine the effect of the location parameter on the results accuracy. The location parameter plays a significant role in determining the stress at point A, as shown in Table 7, in MFS a slight change in this parameter will have a significant impact on the results. Based on the results of this example, it can be concluded that MFS is less efficient than BEM, especially with a small number

Table 5: Comparison of stress values for a plate with much deeper hole at point A.

Node	$\sigma_{x(BEM)}$		
	Linear	Quadratic	$\sigma_{x(MFS)}$
53	570.0	901.2	496.27
111	762.7	765.2	749.0
213	780.2	780.5	786.3
Reference solution	768.3	768.3	786.3

Table 6: Comparison of stress values for a plate with a deep hole at point B.

Node	$\sigma_{x(BEM)}$			$\sigma_{y(BEM)}$			$\tau_{xy(BEM)}$		
	Linear	Quadratic	$\sigma_{x(MFS)}$	Linear	Quadratic	$\sigma_{y(MFS)}$	Linear	Quadratic	$\tau_{xy(MFS)}$
53	131.2	135.06	120.33	138.7	152.10	62.98	59.9	67.8	29.96
111	135.6	135.96	134.50	149.1	150.52	140.5	67.3	68.4	64.00
213	135.8	135.98	135.98	150.1	150.50	148.9	68.1	68.3	68.10
Reference	139.6	139.6	139.6	152.5	152.5	152.5	71	71	71

Table 7: Comparison of stress values of a plate with much deeper hole at point A for different location parameter values.

Location parameter of source points	$\sigma_{x(MFS)}$
0.89	63.93
0.85	538.69
0.82	107.98
0.80	438.23
0.70	638.35
0.67	598.12
0.64	280.41

of collocation and source points where it may be physically impossible to achieve a proper arrangement satisfying the location parameters constraint. However, BEM does not have this limitation and is therefore able to provide more accurate results in this regard, particularly when quadratic elements are used.

4 CONCLUSION

In this study, BEM and MFS were compared with regard to potential problems and elasticity problems. The efficiency of the two proposed methods was assessed over a variety of boundary domains, including simple and concave boundaries. The major challenge facing MFS is to arrange source points and collocation points in such a way that reliable results will be obtained. A location parameter was defined to determine the optimal location of source points relative to each other and the boundary of the problem. According to the results, both methods provide accurate results for simple geometry. In complex geometries, such as in concave domains (where stress concentration is high), the MFS is not as effective as it should be. With such a small number of source points, it is not possible to satisfy the location parameter and reach the desired location parameter. Therefore, the results of the analysis are unreliable. Despite this, BEM has the potential to provide accurate results, even if the geometry of the problem is complex, and quadratic elements will enhance this accuracy. Since input data preparation in both proposed methods occur only at the boundary of the problem, it can be concluded that BEM and MFS reduce simulation time and input data compared to domain types of the problem such as the finite element method.

REFERENCES

[1] Yokoyama, M. & Kanoh, T., Accuracy estimation of the three-D BEM analysis of elastostatic problems by the zooming method. *Advances in Engineering Software*, **31**, pp. 355–365, 2000.
[2] Cheng, A.H. & Hong, Y., An overview of the method of fundamental solutions: Solvability, uniqueness, convergence, and stability. *Engineering Analysis with Boundary Elements*, pp. 118–152, 2020.
[3] Hematiyan, M., Haghighi, A. & Khosravifard, A., A two-constraint method for appropriate determination of the configuration of source and collocation points in the method of fundamental solutions for 2D Laplace equation. *Advances in Applied Mathematics and Mechanics*, 2017.
[4] Drombosky, T.W., Meyer, A.L. & Ling, L., Applicability of the method of fundamental solutions. *Engineering Analysis with Boundary Elements*, **33**(5), pp. 637–643, 2009.
[5] Askour, O., Tri, A., Braikat, B., Zahrouni, H. & Potier-Ferry, M., Method of fundamental solutions and high order algorithm to solve nonlinear elastic problems. *Engineering Analysis with Boundary Elements*, **89**, pp. 25–35, 2018.
[6] Wang, F., Fan, C.M., Hua, Q. & Gu, Y., Localized MFS for the inverse Cauchy problems of two-dimensional Laplace and biharmonic equations. *Applied Mathematics and Computation*, **364**, 124658, 2020.
[7] Jaswon, M., Integral equation methods in potential theory. I. *Proceedings of the Royal Society of London Series A Mathematical and Physical Sciences*, **275**(1360), pp. 23–32, 1963.
[8] Symm, G., Integral equation methods in potential theory. II. *Proceedings of the Royal Society of London Series A Mathematical and Physical Sciences*, **275**(1360), pp. 33–46, 1963.
[9] Rizzo, F. & Shippy, D., A boundary integral approach to potential and elasticity problems for axisymmetric bodies with arbitrary boundary conditions. *Mechanics Research Communications*, **6**(2), pp. 99–103, 1979.
[10] Muskhelishvili, N. et al., *Some Basic Problems of the Mathematical Theory of Elasticity*, vol. 15. Noordhoff Groningen, 1953.
[11] Kupradze, V., Potential methods in elasticity theory. Technical report, Foreign Technology Div Wright-Patterson AFB Ohio, 1967.
[12] Kupradze, V.D. & Aleksidze, M.A., The method of functional equations for the approximate solution of certain boundary value problems. *USSR Computational Mathematics and Mathematical Physics*, **4**(4), pp. 82–126, 1964.
[13] Mathon, R. & Johnston, R.L., The approximate solution of elliptic boundary-value problems by fundamental solutions. *SIAM Journal on Numerical Analysis*, **14**(4), pp. 638–650, 1977.

[14] Karageorghis, A. & Fairweather, G., The method of fundamental solutions for the solution of nonlinear plane potential problems. *IMA Journal of Numerical Analysis*, **9**(2), pp. 231–242, 1989.
[15] Fam, G.S. & Rashed, Y.F., The method of fundamental solutions applied to 3D structures with body forces using particular solutions. *Computational Mechanics*, **36**(4), pp. 245–254, 2005.
[16] Young, D., Tsai, C.C., Chen, C. & Fan, C.M., The method of fundamental solutions and condition number analysis for inverse problems of Laplace equation. *Computers and Mathematics with Applications*, **55**(6), pp. 1189–1200, 2008.
[17] Marin, L., Karageorghis, A. & Lesnic, D., The MFS for numerical boundary identification in two-dimensional harmonic problems. *Engineering Analysis with Boundary Elements*, **35**(3), pp. 342–354, 2011.
[18] Karageorghis, A., Lesnic, D. & Marin, L., A survey of applications of the MFS to inverse problems. *Inverse Problems in Science and Engineering*, **19**(3), pp. 309–336, 2011.
[19] Fan, C.M. & Li, P.W., Numerical solutions of direct and inverse stokes problems by the method of fundamental solutions and the Laplacian decomposition. *Numerical Heat Transfer, Part B: Fundamentals*, **68**(3), pp. 204–223, 2015.
[20] Mohammadi, M., Hematiyan, M.R. & Shiah, Y., An efficient analysis of steady-state heat conduction involving curved line/surface heat sources in two/three-dimensional isotropic media. *Journal of Theoretical and Applied Mechanics*, **56**(4), pp. 1123–1137, 2018.
[21] Gorzelańczyk, P. & Kołodziej, J.A., Some remarks concerning the shape of the source contour with application of the method of fundamental solutions to elastic torsion of prismatic rods. *Engineering Analysis with Boundary Elements*, **32**(1), pp. 64–75, 2008.
[22] Berger, J.R. & Karageorghis, A., The method of fundamental solutions for layered elastic materials. *Engineering Analysis with Boundary Elements*, **25**(10), pp. 877–886, 2001.
[23] Karageorghis, A., A practical algorithm for determining the optimal pseudo-boundary in the method of fundamental solutions. *Adv. Appl. Math. Mech.*, **1**(4), pp. 510–528, 2009.
[24] Li, M., Chen, C. & Karageorghis, A., The MFS for the solution of harmonic boundary value problems with non-harmonic boundary conditions. *Computers and Mathematics with Applications*, **66**(11), pp. 2400–2424, 2013.
[25] Alves, C.J., On the choice of source points in the method of fundamental solutions. *Engineering Analysis with Boundary Elements*, **33**(12), pp. 1348–1361, 2009.
[26] Liu, C.S., An equilibrated method of fundamental solutions to choose the best source points for the Laplace equation. *Engineering Analysis with Boundary Elements*, **36**(8), pp. 1235–1245, 2012.
[27] Wang, F., Liu, C.S. & Qu, W., Optimal sources in the MFS by minimizing a new merit function: Energy gap functional. *Applied Mathematics Letters*, **86**, pp. 229–235, 2018.
[28] Cisilino, A.P. & Sensale, B., Application of a simulated annealing algorithm in the optimal placement of the source points in the method of the fundamental solutions. *Computational Mechanics*, **28**(2), pp. 129–136, 2002.
[29] Jopek, H. & Kołodziej, J., Application of genetic algorithms for optimal positions of source points in the method of fundamental solutions. *Comput. Assist. Mech. Eng. Sci.*, **15**(3–4), pp. 215–224, 2008.
[30] Chen, C., Karageorghis, A. & Li, Y., On choosing the location of the sources in the MFS. *Numerical Algorithms*, **72**, pp. 107–130, 2016.

[31] Hematiyan, M., Arezou, M., Dezfouli, N.K. & Khoshroo, M., Some remarks on the method of fundamental solutions for two-dimensional elasticity. *Comput. Model Eng. Sci. (CMES)*, **121**, pp. 661–686, 2019.
[32] Tadeu, A., Godinho, L. & Chen, C., Performance of the BEM, MFS, and RBF collocation method in a 2.5 d wave propagation analysis. *WIT Transactions on Modelling and Simulation*, vol. 39, WIT Press: Southampton and Boston, 2005.
[33] Salgado-Ibarra, E.A., Boundary element method (BEM) and method of fundamental solutions (MFS) for the boundary value problems of the 2-D Laplace's equation, 2011.
[34] Alves, C.J., Martins, N.F. & Valtchev, S.S., Trefftz methods with cracklets and their relation to BEM and MFS. *Engineering Analysis with Boundary Elements*, **95**, pp. 93–104, 2018.
[35] Ahmed, M.T., Lavers, J. & Burke, P., An evaluation of the direct boundary element method and the method of fundamental solutions. *IEEE Transactions on Magnetics*, **25**(4), pp. 3001–3006, 1989.
[36] Nath, D. & Kalra, M., Solution of Grad–Shafranov equation by the method of fundamental solutions. *Journal of Plasma Physics*, **80**(3), pp. 477–494, 2014.
[37] Godinho, L., Costa, E., Pereira, A. & Santiago, J., Some observations on the behavior of the method of fundamental solutions in 3D acoustic problems. *International Journal of Computational Methods*, **9**(04), 1250049, 2012.
[38] Godinho, L. & Soares Jr, D., Frequency domain analysis of interacting acoustic–elastodynamic models taking into account optimized iterative coupling of different numerical methods. *Engineering Analysis with Boundary Elements*, **37**(7–8), pp. 1074–1088, 2013.
[39] Dyhoum, T., Lesnic, D. & Aykroyd, R., Solving the complete-electrode direct model of ERT using the boundary element method and the method of fundamental solutions. *Electronic Journal of Boundary Elements*, **12**(3), 2014.
[40] Liravi, H., Arcos, R., Ghangale, D., Noori, B. & Romeu, J., A 2.5 D coupled FEM-BEM-MFS methodology for longitudinally invariant soil-structure interaction problems. *Computers and Geotechnics*, **132**, 104009, 2021.
[41] Paris, F. & Canas, J., *Boundary Element Method: Fundamentals and Applications*, Oxford University Press: USA, 1997.
[42] Sadd, M.H., *Elasticity: Theory, Applications, and Numerics*, Academic Press, 2009.
[43] Gao, X.W. & Davies, T.G., *Boundary Element Programming in Mechanics*, Cambridge University Press, 2002.